

BETA-DECAY ENERGIES AND MASSES OF NEUTRON-DEFICIENT RUBIDIUM AND CAESIUM ISOTOPES

J. M. D'Auria⁺, J. W. Grüter⁺⁺, L. Westgaard
CERN, Geneva, Switzerland

G. Nyman, P. Peuser, E. Roeckl
GSI, Darmstadt, Fed. Rep. Germany

H. Otto
Institut für Kernchemie, Universität Mainz, Fed. Rep. Germany
and
The ISOLDE Collaboration, CERN, Geneva, Switzerland

Abstract

Total beta-decay energies were measured by a beta-gamma coincidence method for ^{76}Rb , ^{78}Rb , ^{118}Cs , ^{120}Cs and ^{122}Cs . The resulting Q values and masses together with experimental data from the literature are compared with mass formulae, with particular emphasis on Kr and Rb isotopes in the $N=Z$ region.

1. Introduction

In studying nuclei far away from stability the mass excesses of nuclear ground states are of particular interest, because information on nuclear binding of an ensemble of nucleons away from the stable configuration can be obtained. Another obvious motivation for mapping the mass surface away from stability is that extrapolation into still more exotic regions is facilitated, thus laying the ground for more detailed experiments on these nuclei.

Both the numerous reaction studies¹⁾ and the application of on-line mass spectrometry²⁾ have yielded the determination of precise masses for a considerable number of far-unstable nuclei. In spite of being less accurate, the measurement of mass differences from decay energies, on the other hand, is a valuable method in view of the limitations of the former ones, which have so far been restricted to light or not too far unstable nuclei in the one case, to alkali-element isotopes in the other.

Using mass-separated sources from the ISOLDE on-line isotope facility several mass and decay-energy measurements³⁻⁸⁾ of moderate precision have been carried out, most recently for a number of neutron-deficient Rb and Cs isotopes as well as for some neutron-rich Fr and Ra isotopes^{9,10)}. The isobaric mass differences obtained from beta-end-point measurements are compared to the corresponding increment of the mass surface from model calculations. Alternatively, the ground state masses themselves can be compared in case they are obtainable from addition of mass differences.

⁺ On sabbatical leave from Simon Fraser University, Burnaby, B. C., Canada.

⁺⁺ On leave from Institut für Kernphysik, KFA Jülich, Fed. Rep. Germany

In a previous work^{9,10)} we measured Q values of neutron-deficient Rb isotopes and incorporated them into a mass systematics of Rb and Kr isotopes. The increased binding towards the $N=Z$ line was interpreted as being due to the Wigner symmetry energy. The experimental masses of the odd nuclei ^{76}Rb and ^{78}Rb fell below the smooth systematics.

In the present paper we give the preliminary results of a new series of beta-gamma coincidence experiments for ^{76}Rb , ^{78}Rb , ^{118}Cs , ^{120}Cs and ^{122}Cs , thus covering some of the nuclei studied earlier as well as extending further towards more neutron-deficient Cs isotopes. We also describe the measurement of the response function of the telescope detector used to measure beta-ray spectra. Q values and masses resulting from preliminary evaluations of these data are presented and compared with recent results from direct mass measurements and with predictions from mass formulae.

2. Calibration of beta-detectors for Q-value measurements

2.1 Beta-detector telescope.

A telescope was designed for measuring Q-values up to 15 MeV of short-lived isotopes at an on-line isotope separator. It consists of an 8 mm ϕ x 0.5 mm NE 102A plastic scintillator as energy-loss detector and a 7.6 cm ϕ x 7.6 cm NUPLEX plastic scintillator for energy analysis. The thick detector is cone-shaped at one end in order to fit onto a 5.1 cm ϕ RCA 8850 photomultiplier. For energy analysis signals from the thick plastic detector are stored in fast-slow triple coincidence with single-channel analyzer signals from both plastic detectors and signals from a time-to-pulse height converter measuring the time distribution (usually about 2 nsec FWHM) between the two detectors. At an expense of an energy loss of about 100 keV for electrons between 1 and 10 MeV, the energy-loss detector serves for gamma rejection and defines the solid angle for a point source close to the telescope in a way that large entrance angles (corresponding to smaller effective thicknesses of the energy detector) are avoided.

Moreover, in order to explore the applicability of thick Ge(Li) or ultrapure Ge detectors for Q-value measurements, a 12.5 cm² x 12 mm thick Ge(Li)

detector was tested in combination with a 32 mm ϕ x 0.5 mm NE 102A plastic scintillator as energy loss detector. The Ge(Li) detector was mounted on a cold finger for liquid nitrogen cooling and was separated by a 30 μ m aluminium foil from the thin plastic detector.

2.2 Definition of the response function.

The response function $R(E, E')$ describes the probability of detecting a beta particle of energy E' in the detector at an energy E , and is connected to the efficiency $\epsilon(E')$ via

$$\int_0^{\infty} R(E, E') dE = \epsilon(E') \quad (1)$$

Applied to the measurement of a beta spectrum $S_0(E')$, the experimental spectrum $S(E)$ results from folding $S_0(E)$ with the response function.

$$S(E) = \int_0^{\infty} R(E, E') S_0(E') dE' \quad (2)$$

$R(E, E')$ characterizes a certain detector system including the source-detector geometry.

2.3 Measurement of the response function.

Response functions for the plastic scintillator telescope as well as for the plastic Ge(Li) telescope were measured using mono-energetic e^- beams in the energy range from 1 to 7 MeV from the beta spectrometer on-line to the FRM reactor at Garching, and in the energy range from 4 to 15 MeV from the betatron at the Physikalisches Institut der Universität Würzburg. The energy spread of the beams amounted to 1% in both cases. The results presented here refer to the betatron measurements exclusively. The response of the plastic telescope to e^+ particles has been measured at the Compton spectrometer of the LINAC at MPI für Chemie, Mainz (energy spread 1.5%).

Fig. 1 shows examples of the pulse height distributions obtained for 10 MeV e^- and e^+ beams directed centrally along the telescope axis. Normalizing these pulse-height spectra to the total number of potentially contributing beta particles, which were measured simultaneously by counting the signals from the energy-loss detector, yields the corresponding response function. Since measurements under inclined beam directions have not yet been completed, we assume in the following these "axial" response functions to be approximately representative for a point source geometry.

2.4 Analysis and discussion of response functions.

The experimental response functions are fitted as suggested by Schüpferling¹¹⁾ by a least-squares fit yielding besides the total efficiency the following energy-dependent parameters: center and width of the full-energy Gaussian peak, area and exponential constants of the low energy tail. As an example, results from fits to the experimental response functions for e^- beams on the plastic telescope are shown in fig. 2. Extension of these investigations are in progress¹²⁾ with the aim of determining the energy-dependent response function $R(E, E')$ for e^- , e^+ point sources with both telescopes, allowing the unfolding of the experimental beta spectra according to eq. (2).

The simple extrapolation of the high-energy end of the positron spectra as discussed in section 3) relies on the following results of the calibration measurements¹²⁾, which were determined for axial e^- beams and are supposed to approximately hold for e^+ point-sources also:

- 1) The integral nonlinearity between 4 and 15 MeV amounts to 1%.
- 2) The high values (94%) of the total efficiency and its weak dependence on energy support the assumption that the experimental beta spectra are not strongly distorted.

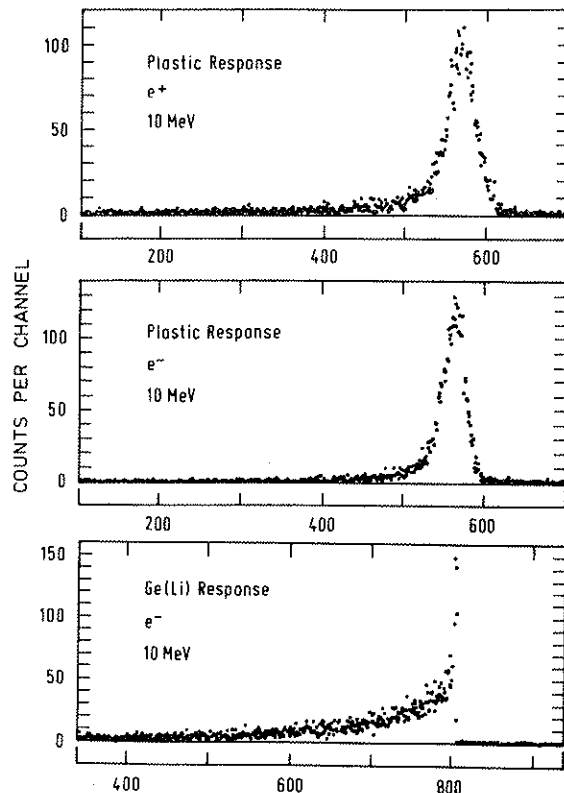


Fig. 1 Examples of the pulse-height distributions measured for 10 MeV monoenergetic e^- and e^+ beams impinging axially on a plastic-scintillator telescope or a combined plastic-Ge(Li) telescope. **Top:** e^+ beam, 8 mm ϕ x 0.5 mm energy-loss detector (plastic scintillator), 7.5 cm ϕ x 7.5 cm energy detector (plastic scintillator). **Middle:** e^- beam, 8 mm ϕ x 0.5 mm energy-loss detector (plastic scintillator), 7.5 mm ϕ x 7.5 cm energy detector (plastic scintillator). **Bottom:** e^- beam, 0.5 mm energy-loss detector, 12.5 cm² x 12 mm Ge(Li) energy detector.

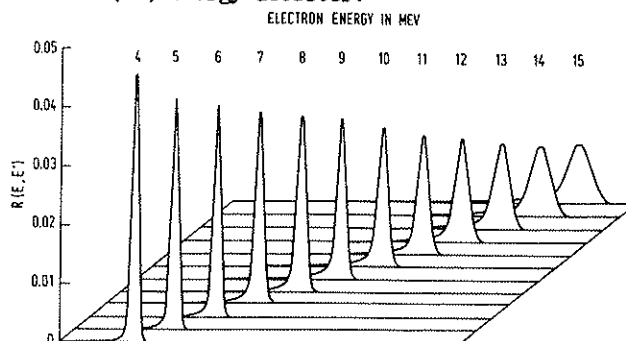


Fig. 2 Isomeric plot of the response functions of the plastic scintillator telescope to monoenergetic axial e^- beams between 4 and 15 MeV.

3. Q-value measurements

3.1 Experimental technique.

Isotopes of Rb and Cs were produced at the ISOLDE-2 facility¹³⁾ by bombarding targets of Y and La, respectively, with 600 MeV protons from the CERN synchrocyclotron. After surface ionization the ions were extracted, mass separated and transported via an ion-optical transfer line to the collector position of a moving-tape station. Collection, waiting and counting intervals were chosen according to the isotope (isomer) in question and to source-strength limitations due to pile-up. At the counting position of the moving-tape station, a Ge(Li) detector and the plastic scintillator telescope described in section 2.1 face the tape (see fig. 3). The energy calibration of the telescope was based on the conversion-electron lines of ¹³⁷Cs and ²⁰⁷Pb sources (taking into account the energy losses in windows and in the thin detector) and on the known linearity of the telescope. The ²⁰⁷Pb calibrations interspersed regularly between the data-taking runs and a pulser was used to check the stability of the calibration.

The linear signals from the two detectors were fed into two ADCs (1024 channels for the beta spectra) connected to an HP 2100 computer where the coincidence events were buffered as a two-dimensional matrix. The coincidences as well as the singles spectra were written onto magnetic tape. Digital windows on prominent gamma-lines (as well as on background) were set off-line in order to obtain the spectra of beta-decay feeding known levels.

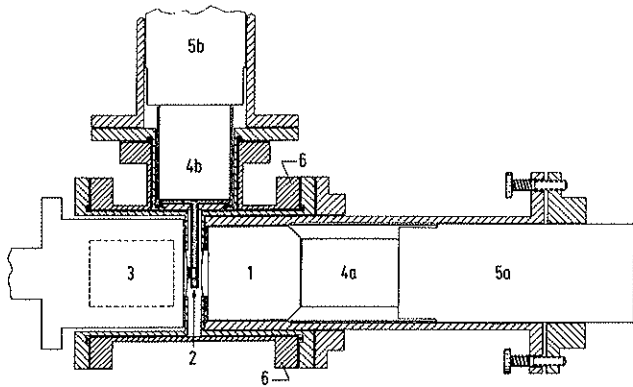


Fig. 3 Beta-gamma detector system. 1) Thick plastic scintillator. 2) Thin plastic scintillator close to the tape. 3) Ge(Li) detector. 4 a,b) Photomultiplier. 5 a,b) Photomultiplier base. 6) Vacuum chamber of the tape station.

3.2 Data analysis.

In the absence of the complete response function for an unfolding procedure, Fermi-Kurie (FK) plots of the gamma-coincident beta spectra were preliminarily fitted by hand. The validity of this rough evaluation method can be checked by investigating the known positron spectra of ⁶⁰Ga and ⁸⁰Rb. ⁶⁰Ga with a Q_{EC} value of 5175 ± 3 keV decays by 91% to the ⁶⁰Zn ground state with an endpoint energy of 4153 ± 3 keV. (For Q values and other decay data see ref. 10, if not stated otherwise.) For the endpoint energy of the positron spectrum in coincidence with annihilation radiation (Fig. 4) we determine

4180 ± 300 keV from a FK plot in the energy range 3.2 to 4.2 MeV, in agreement with the literature value.

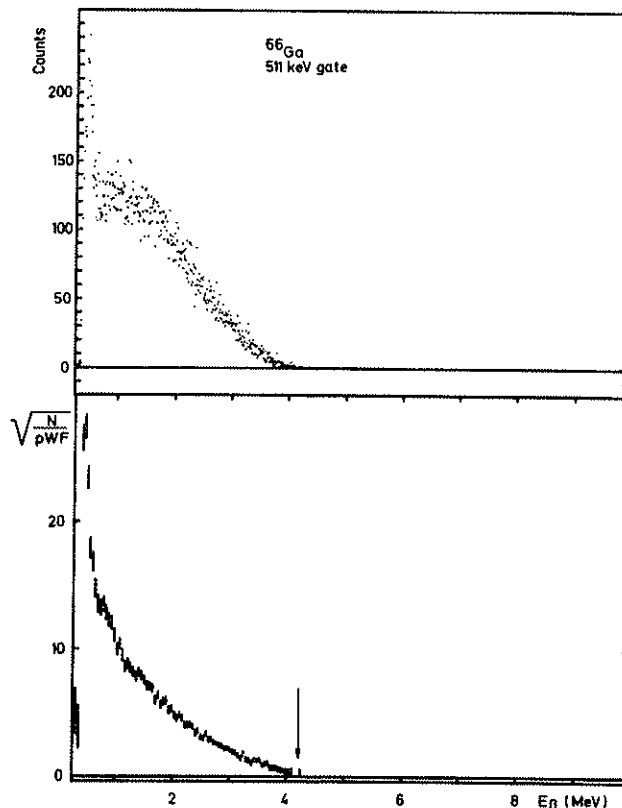


Fig. 4 Positron spectrum (top) of ⁶⁶Ga in coincidence with annihilation radiation. The arrow indicates the endpoint energy deduced from the FK analysis (bottom).

Another comparison with a known Q value was made using ⁸⁰Rb sources produced on-line at the ISOLDE-2 separator. The positron spectrum in coincidence with the 617 keV ($2^+ \rightarrow 0^+$) transition in ⁸⁰Kr is shown in Fig. 5. Fitting the FK plot in the energy range 1.4 to 4.1 MeV leads to an endpoint energy of 4040 ± 300 keV or a Q_{EC} value of 5680 ± 300 keV in agreement with the literature value of 5701 ± 22 keV.

3.3 The decay of 37 sec ⁷⁶Rb.

In addition to known gamma lines¹⁰⁾ a new gamma line of 2573 keV was recently assigned¹⁴⁾ to the ⁷⁶Rb decay. The positron-coincident intensity of this line amounts to about 70% of that of the 423 keV ($2^+ \rightarrow 0^+$) transition. Since gamma-gamma coincidence measurements¹⁴⁾ show that the 2573 keV line is accompanied by a few weak gamma rays only we assume predominant feeding of a 2573 keV level, decaying directly to the ground state. In Fig. 6 the positron spectrum of ⁷⁶Rb in coincidence with the 2573 keV gamma line is shown. The FK analysis of this spectrum gave an endpoint energy of 4740 ± 400 keV, corresponding to a Q_{EC} value of 8340 ± 400 keV. This result is higher by about 1.7 MeV than the corresponding value found previously¹⁰⁾. This

difference can be understood by considering the weak high-energy tail in the 423 keV-gated spectrum, which was neglected in the previous evaluation.

an oversimplified analysis of a composite beta spectrum.

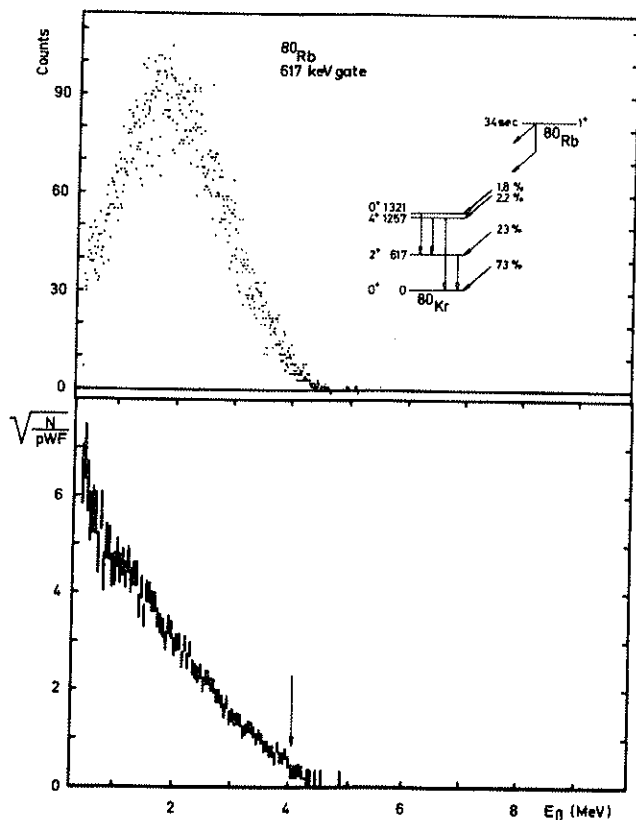


Fig. 5 Positron spectrum (top) of ^{80}Rb in coincidence with the 617 keV line. The decay scheme shown in the inset is from ref. 10. The arrow indicates the endpoint energy deduced from the FK analysis (bottom).

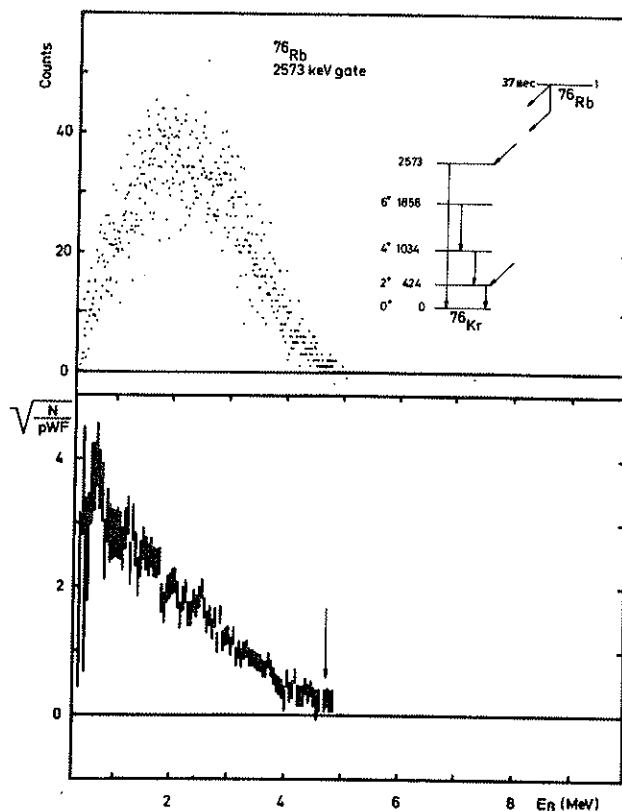


Fig. 6 Positron spectrum (top) of ^{76}Rb in coincidence with the 2573 keV gamma line and the corresponding FK plot (bottom). The decay scheme shown in the inset is from refs. 10 and 14, the spin value of 1 for ^{76}Rb comes from a recent measurement of Fischer et al. 15) The arrow indicates the endpoint energies of 4750 ± 400 keV deduced from the FK analysis.

3.4 The decay of 6 min and 17 min ^{78}Rb .

The presence of two beta-decaying states, of half-lives 6 min for the metastable and 17 min for the ground state, makes the interpretation of the ^{78}Rb beta-gamma coincidence data difficult. From recent ABMR experiments 16) the spin value 4 (metastable state) and 0 (ground state) have been determined. We discuss here only the result of the beta-gamma measurement timed to emphasize the decay of the ground-state (waiting time 30 min between collection and counting). Gates on low-energy gamma rays like the 455 keV ($2^+ \rightarrow 0^+$) or the 664 keV ($4^+ \rightarrow 2^+$) transition may seem to support previous results 10), but there is also an indication for different components in the beta spectra. In spite of the poor statistics, an endpoint energy of 2200 ± 400 keV has been determined for the beta spectrum in coincidence with the 3438 keV gamma-ray (see Fig. 7), whose positron-coincident intensity is about 16% of that of the 424 keV ($2^+ \rightarrow 0^+$) transition. This puts a lower limit of 6600 keV on the ^{78}Rb Q_{EC} value. Identifying the gate transition with the 3438.2 keV gamma ray, observed by the McGill group 17) to feed the 2^+ level at 455 keV, gives a Q_{EC} value of 7100 ± 400 keV for ^{78}Rb . This is again about 1.6 MeV higher than previously reported 10), the discrepancy presumably, as in the ^{76}Rb case, being due to

3.5 The decay of 21 sec and 4.2 min ^{122}Cs .

As with ^{78}Rb the decay of ^{122}Cs is also obscured due to isomerism. As can be seen from the beta-coincident gamma spectra, the 21 sec state (spin 1 (ref. 16), presumably ground state) decays predominantly via the 331 keV ($2^+ \rightarrow 0^+$) transition, whereas the 4.2 min state (spin 8 (ref. 16)) feeds additional levels decaying by the 750 keV ($8^+ \rightarrow 6^+$), 639 keV ($6^+ \rightarrow 4^+$) and 497 keV ($4^+ \rightarrow 2^+$) gamma transitions. Beta spectra gated with the 331 keV transition in ^{122}Xe have been recorded under different timing conditions in order to emphasize one or the other of the isomers. For the short-lived (ground) state the FK analysis shows a predominant component with the endpoint energy 5.7 ± 0.4 MeV which gives a Q_{EC} value of 7.1 ± 0.4 MeV. On the other hand, the FK analysis of the long-lived component, gated with the 331 keV gamma line contains clearly different components. The most energetic one has an endpoint energy of 6.14 ± 0.5 MeV corresponding to a Q_{EC} value of 7.5 ± 0.5 MeV.

3.6 The decays of 58 sec ^{120}Cs and 16.4 sec ^{118}Cs .

Beta spectra for ^{120}Cs in coincidence with the 320 keV ($2^+ \rightarrow 0^+$) transition, and for ^{118}Cs in coinci-

dence with the 337 keV ($2^+ \rightarrow 0^+$) transition are shown in Figs. 8 and 9, respectively. In spite of the complexity of the gated spectra shown, fits were attempted to the high-energy end of these spectra, yielding an endpoint energy of 6.5 ± 1.0 MeV and a Q_{EC} value of 7.8 ± 1.0 MeV for ^{120}Cs , and an endpoint energy of 8.0 ± 1.0 MeV and a Q value of 9.3 ± 1.0 MeV for ^{118}Cs .

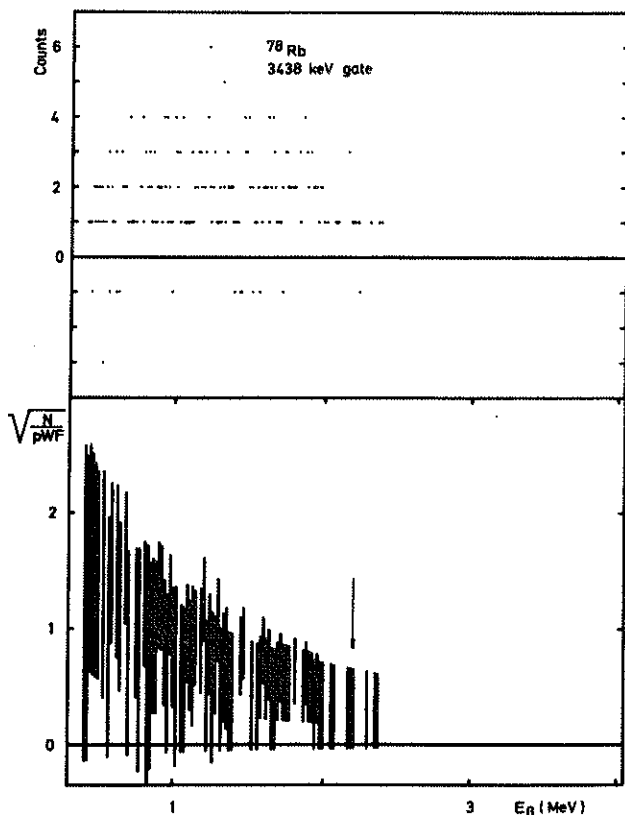


Fig. 7 Positron spectrum (top) of ^{78}Rb in coincidence with the 3438 keV gamma line. The arrow indicates the endpoint energy of 2200 ± 400 keV deduced from the FK analysis (bottom).

4. Discussion

Table 1 compiles the experimental Q_{EC} values from the present work as well as a comparison to the Seeger-Howard mass formula¹⁹.

Table 1

Nuclide	$T_{1/2}$	Q_{EC} (MeV)	
		Exp.	Calc. (ref. 19)
^{76}Rb	37 sec	8.34 ± 0.40	8.56
^{78}Rb	17 min	7.12 ± 0.40	7.10
^{118}Cs	16,4sec	9.3 ± 1.0	8.97
^{120}Cs	58 sec	7.8 ± 1.0	7.84
^{122}Cs	21 sec	7.05 ± 0.40	6.71

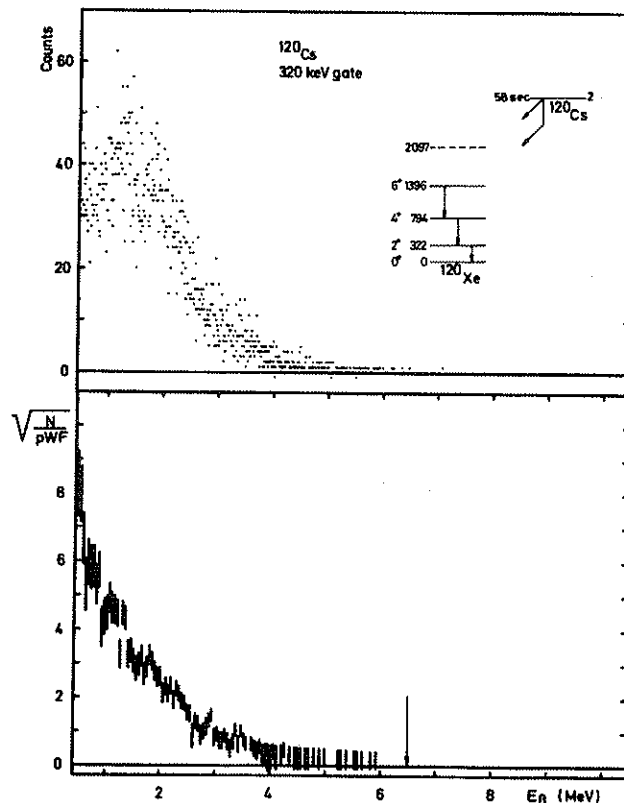


Fig. 8 Positron spectrum (top) of ^{120}Cs in coincidence with 320 keV gamma line. The decay scheme shown in the inset is from this work and refs. 16, 18. The arrow indicates the endpoint energy of 6.5 ± 1.0 MeV deduced from the FK analysis (bottom).

It is tempting to update already now the mass systematics for Rb isotopes, with respect to the earlier version¹⁰, including the corrected but preliminary experimental Q_{EC} values of ^{76}Rb and ^{78}Rb as well as the estimate²¹ for the Q_{EC} value of the newly discovered $N=Z$, $T=1$, nucleus ^{74}Rb . In Fig. 10 the Rb masses are plotted as an excess over a smooth liquid-drop mass²⁰ containing the usual volume, surface, quadratic symmetry and Coulomb terms and the odd-even term but not the shell correction term. Inclusion of shell correction in the mass formula of Myers and Swiatecki²⁰ accounts well for the $N=50$ shell effect but not for the increased binding energy of nuclei in the $N=Z$ region. The recent liquid-drop model calculation of Seeger and Howard¹⁹ including Strutinsky-normalized shell and deformation corrections represents well both the shell effect and the increased binding around the $N=Z$ line.

As can be seen from Fig. 11, the latter agreement is considerably improved compared to the earlier work¹⁰ by including the new ^{74}Rb , ^{76}Rb and ^{78}Rb masses, which supports form and magnitude of the Wigner symmetry energy contained in the Seeger-Howard mass formula (see also refs. 9, 10). The recent results from direct mass measurements obtained by the Orsay group²² fit also nicely into this picture. The discussion in ref. 10 of the possible reasons for an increased binding in ^{76}Rb and ^{78}Rb was obviously based upon erroneous experimental Q values.

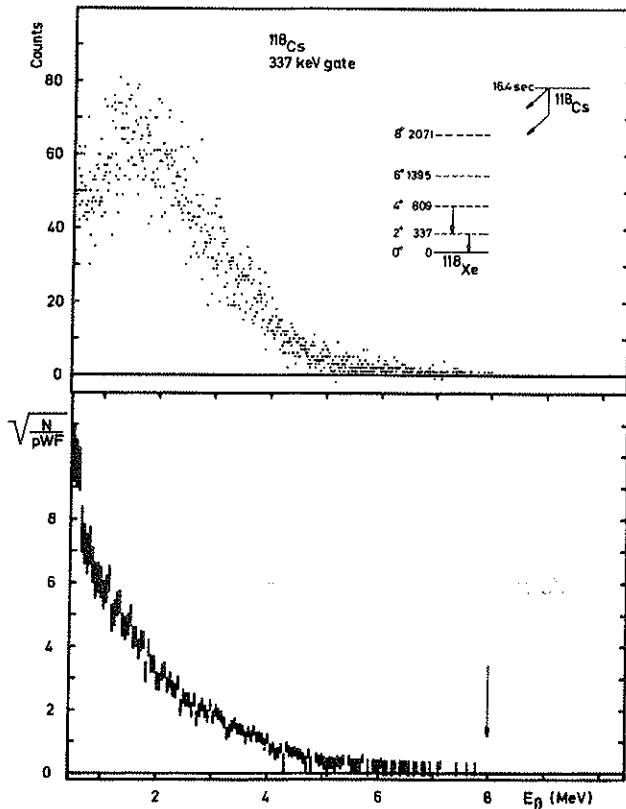


Fig. 9 Positron spectrum of (top) ^{118}Cs in coincidence with the 337 keV gamma line. The decay scheme shown in the inset is from this work and from ref. 18. The arrow indicates the endpoint energy of 8.0 ± 1.0 MeV deduced from the FK analysis (bottom).

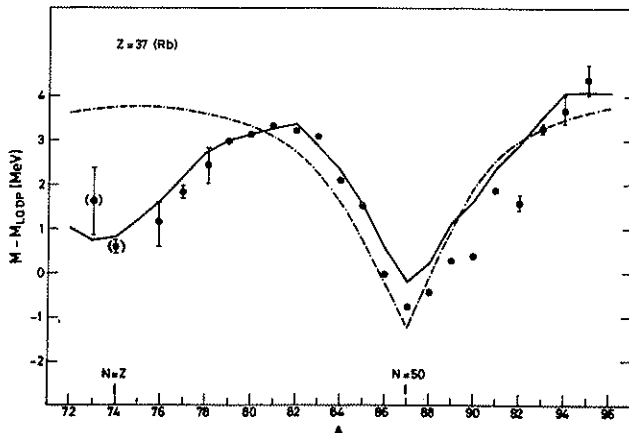


Fig. 10 Experimental (black dots) and calculated masses of Rb isotopes after subtraction of a smooth liquid-drop term²⁰. The calculated masses are from Myers and Swiatecki²⁰ (dashed curve) and from Seeger and Howard¹⁹ (full-drawn curve).

5. Outlook

For ^{73}Rb and ^{74}Rb the "experimental" Q values and masses given above were deduced from systematics of the Coulomb displacement energy^{10,19}). Even though the plastic-scintillator telescope can at present hardly compete with the estimated precision of the above systematics, it is challenging to try extension of endpoint measurement up to energies of the order of 10 MeV. A determination of such a Q_{EC} value with an accuracy of a few hundred keV may in many situations represent valuable information.

The present work evidently represents a status report of an experiment in progress, and more detailed spectroscopy is required especially for high energy gamma transitions and in the cases of isomerism. The measurement of Q values, which has so far been widely used for mass determination by consecutive addition starting from known masses near the stability line may on the other hand even gain in interest in cases where precise masses far away from stability are available from direct (mass spectrometric) measurements.

References.

- 1) Atomic Masses and Fundamental Constants Σ , editors: I.H.Sanders and A.H.Wapstra, Plenum Press, 1976.
- 2) C.Thibault, R. Klapisch, C.Rigaud, A.M.Poskanzer, L.Lessard and W.Reisdorf, Phys.Rev.C10 (1975) 1181.
- 3) E.Beck, Thesis, Ruprecht-Karl Universität, Heidelberg (1969) and Nucl. Instr. Meth. 76 (1969) 77.
- 4) E.Beck, in Proc. Int. Conf. on the Properties of Nuclei Far From the Region of Beta-Stability, Leysin, 1976, CERN 70-30 (1970) Vol. 1, p. 353.
- 5) A. Lindahl, O.B. Nielsen, and I.L. Rasmussen, in Proc. Int. Conf. on the Properties of Nuclei Far From the Region of Beta-Stability, Leysin, 1976, CERN 70-30 (1970), Vol. 2, p. 331.
- 6) L.Westgaard, I.Zylicz and O.B. Nielsen, in Atomic Masses and Fundamental Constants Σ , editors: I.H. Sanders and A.H.Wapstra, Plenum Press, 1972, p.94.
- 7) B.R.Erdal, L.Westgaard, J.Zylicz and E.Roeckl, Nucl. Phys. A 194 (1972) 449.
- 8) E.Roeckl, D.Lode, K.Bächmann, B.Neidhart, G.K.Wolf, W.Lauppe, N.Kaffrell and P.Patzelt, Z.Physik 266 (1974) 65.
- 9) K.Aleklett, G. Nyman, E.Roeckl and L.Westgaard, in ref. 1, p. 88.
- 10) L.Westgaard, K.Aleklett, G.Nyman and E.Roeckl, Z.Physik A 275 (1975) 127.
- 11) H.M. Schüpferling, Nucl.Instr.Meth. 123 (1975) 67.
- 12) G.Nyman, P.Peuser, E.Roeckl, W.Lauppe, D.Protic and H.Otto, to be published.
- 13) H.L. Ravn, S. Sundell and L.Westgaard, Nucl. Instr. Meth. 123 (1975) 131; and H.L. Ravn, L.C. Carraz, J.Demimal, E.Kugler, M. Skarestad, S. Sundell and L.Westgaard, contribution to the EMIS-9 conference, to be published in Nucl. Instr.Meth.
- 14) J.W.Grüter and E.Nolte, private communication.
- 15) K.Fischer, H.Kremling, H.J.Kluge, R.Neugart, P.Dabkiewicz and E.W.Otten, contribution to this conference.
- 16) S. Ingelman, C.Ekström, G.Wannberg and M.Skarestad, contribution to this conference.
- 17) S.M. Mark and collaboration, private communication.
- 18) Nucl. Data Sheets 17 (1976).
- 19) P.A. Seeger and W.M. Howard, LA-5750 (1974) and Nucl. Phys. A 238 (1975) 491.
- 20) W.D.Myers and W.J. Swiatecki, UCRL-11980 (1965) and Nucl. Phys. 81(1966) 1.
- 21) J.M. D'Auria, L.C. Carraz, P.G. Hansen, B.Jonson, S.Mattson, H.L.Ravn, M.Skarestad and L.Westgaard, contribution to this conference.
- 22) C.Thibault, private communication.